

RESEARCH ARTICLE

Biochemical and histological alterations induced by nickel oxide nanoparticles in the ground beetle *Blaps polychresta* (Forskl, 1775) (Coleoptera: Tenebrionidae)

Saeed El-Ashram^{1,2*}, Awatef M. Ali³, Salah E. Osman³, Shujian Huang¹, Amal M. Shouman³, Dalia A. Kheirallah^{3*}

1 College of Life Science and Engineering, Foshan University, Foshan, Guangdong, China, **2** Faculty of Science, Kafrelsheikh University, Kafr El-Sheikh, Egypt, **3** Department of Zoology, Faculty of Science, Alexandria University, Alexandria, Egypt

* saeed_elashram@yahoo.com, saeed_elashram@fosu.edu.cn (SEA); Daliakheirallah@yahoo.com, daliakheirallah@alexu.edu.eg (DAK)



OPEN ACCESS

Citation: El-Ashram S, Ali AM, Osman SE, Huang S, Shouman AM, Kheirallah DA (2021) Biochemical and histological alterations induced by nickel oxide nanoparticles in the ground beetle *Blaps polychresta* (Forskl, 1775) (Coleoptera: Tenebrionidae). PLoS ONE 16(9): e0255623. <https://doi.org/10.1371/journal.pone.0255623>

Editor: Shawky M. Aboelhadid, Beni Suef University Faculty of Veterinary Medicine, EGYPT

Received: February 21, 2021

Accepted: June 30, 2021

Published: September 24, 2021

Copyright: © 2021 El-Ashram et al. This is an open access article distributed under the terms of the [Creative Commons Attribution License](https://creativecommons.org/licenses/by/4.0/), which permits unrestricted use, distribution, and reproduction in any medium, provided the original author and source are credited.

Data Availability Statement: All relevant data are within the paper and its [Supporting Information](#) files.

Funding: National Key R&D Program of China (2018YFD0501200); Start-up Research Grant Program provided by Foshan University, Foshan city, Guangdong province for distinguished researchers, Guangdong Science and Technology Plan Project (Grant No:1244 0600 4560 7389XC); and School of Life Science and Engineering fund

Abstract

The present study evaluates the effect of nickel oxide nanoparticles on some biochemical parameters and midgut tissues in the ground beetle *Blaps polychresta* as an indicator organism for nanotoxicity. Serial doses of the NiO-NPs colloid (0.01, 0.02, 0.03, 0.04, 0.05, and 0.06 mg/g) were prepared for injecting into the adult beetles. Insect survival was reported daily for 30 days, and the sublethal dose of 0.02 mg/g NiO-NPs was selected for the tested parameters. After the treatment, nickel was detected in the midgut tissues by X-ray microanalysis. The treated group demonstrated a significant increase in aspartate aminotransferase (AST) and alanine aminotransferase (ALT) activities when compared to the untreated group. However, the treated group demonstrated a significant decrease in ascorbate peroxidase (APOX) activity when compared to the untreated group. Histological and ultrastructural changes in the midgut tissues of treated and untreated beetles were also observed. The current findings provide a precedent for describing the physiological and histological changes caused by NiO-NPs in the ground beetle *B. polychresta*.

1. Introduction

The production of nanoparticles has increased due to the instant progress of nanotechnology [1]. With the progress of nanotechnology, metal oxide nanoparticles (MONPs) have been widely used in different fields, for instant paints, cosmetics, electronic devices, additives in food, and medical and biological systems [2, 3]. With the excessive use of MONPs, studies have investigated their adverse effects on the environment, human health, and soil organisms [4]. Derived nanoparticles (NPs) can induce different interactions in living organisms [5].

The size of NPs enables them to reach the cell's nucleus through the nuclear pore and interact directly with the DNA in the chromosomes, causing genetic damage. Also, they can interact with proteins involved in DNA replication and generate high quantities of oxidative stress that induces DNA damage [6].

(Grant No: KLPREAD201801-02). The funders had no role in study design, data collection and analysis, decision to publish, or preparation of the manuscript.

Competing interests: The authors have declared that no competing interests exist.

Nickel (Ni) is combined with some metals to make alloys, such as stainless steel [7]. It is extensively used in industry due to its toughness, hardness, high resistance to corrosion and rusting, and it also has good plasticity [8]. Industrial activities can raise the Ni concentration in the environment [8]. Ni has low solubility in water, which indicates its toxicity effects [9]. Exposure of organisms to Ni or its compounds induces different pathological effects, such as inflammation, allergy reactions, teratogenicity in the human body, lung fibrosis and lung cancer [8]. Nickel nanoparticles (Ni-NPs) are used in biological medicine and may induce cardiac toxicity, liver and spleen injury, and lung inflammation [8].

Insects have the ability to act as environmental monitors in a variety of situations [10]. In addition, insects have a short generation period, are very prolific, are inexpensive, and offer good genetic tools for studying human-related illnesses, such as cancer and tumors [11, 12]. Beetle genetic sequences are accessible, and parts, including the midgut, reproductive organs, and fat bodies, are quite straightforward to access for study [13]. Tenebrionid beetles are excellent ecological models since they live in a variety of environments [14]. Their behavior is inextricably linked to human activities, like urbanization, agricultural areas, and plantations [15]. They're also incredibly adaptable to harsh climatic circumstances, and, unlike other insects, they live for a long time and maintain a steady population [16]. The ground beetle *B. polychresta* (Coleoptera: Tenebrionidae) is the most common tenebrionid and may be seen in enormous numbers [17]. The toxicity of nanoparticles has been studied using zebrafish [18]. Due to its fast embryonic growth, it shows complex behaviors and may be utilized as an animal model under particular physical circumstances (temperature $\leq 28^{\circ}\text{C}$). However, since it needs a low temperature, it might be challenging to utilize as an ecological model at times. As a consequence, the data may be erroneous [19].

Biochemical reactions are the result of an organism's response to a stressor [20]. Biochemical analysis is progressively used in environmental risk assessments to monitor the prevalence of xenobiotics [21]. Therefore, biochemical alterations demonstrate the negative effect that results from vulnerability to a contaminant [22]. The detoxification enzymes in insects are the defence barriers against foreign compounds and they have significant roles in preserving normal physiological functions [23]. Aspartate aminotransferase (AST) and alanine aminotransferase (ALT) aid energy production and serve as a connection between the protein and carbohydrate metabolism [24]. These enzymes are known to be changed during various pathological conditions. The increase in transaminases is considered evidence of cellular leakage and loss of functional cell membrane integrity [23].

Reactive oxygen species (ROS) can damage proteins, lipids, and other important macromolecules in the insect's body. Therefore, organisms must scavenge ROS before cellular damage [25]. Ascorbate peroxidase (APOX) reduces H_2O_2 with concordant ascorbate oxidation [26]. Insects distinctly lack glutathione peroxidase and, since catalase has a poor affinity for H_2O_2 , the APOX enzyme may have a significant role in removing H_2O_2 in insects [27].

The midgut epithelium is the principle site that manages the detoxification of ingested xenobiotics [28]. It is considered an important organ for toxicity analysis because the accumulation of metals occurs in the midgut [29]. Moreover, it is one of the primary interfaces where insects come in contact with injected metals [30]. MO-NPs are capable of inducing cellular and subcellular modifications in the midgut epithelium in insects [31]. Therefore, histological and ultrastructure inspections help in monitoring the pathological effects even at the sublethal level [32].

The current study aims to assess the biochemical, histological, and ultrastructure changes that resulted in the ground beetle *B. polychresta* as a sensitive indicator organism for nickel oxide nanoparticles (NiO-NPs) that may be accumulated in the environment by industrial activities.

2. Materials and methods

Ethics Statement: The ethical rules for animal regulations were followed and approved by the Faculty of Science, Alexandria University committee in January 2014 (Alex-11-2014). All institutional and national Guidelines for the care and use of animals (insects) were followed.

2.1. The studied insect

According to Condamine *et al.* [33], beetles were identified as *Blaps polychresta* in the family Tenebrionidae at the Faculty of Agriculture, Alexandria University, Entomology Department.

2.2. Sampling procedure

One-hundred and forty beetles were sampled from a non-contaminated site, the garden of the Faculty of Science, Elshatby, Alexandria University, Alexandria, Egypt [34].

To guarantee that the area would not be affected, the beetle collection site was situated on private property. They were preserved alive in local soil and plants in glass cages in the laboratory. They were kept at a temperature of $29 \pm 3^\circ\text{C}$ and humidity of 85% RH, similar to their place of origin.

The beetles were divided into seven groups, one untreated group and six treated groups with different nickel oxide nanoparticles (NiO-NPs) concentrations. Each group contained 20 adult beetles.

2.3. Synthesis of nickel oxide

Nickel (II) oxide (NiO) nanopowder [Product No.: 637130, APS: <50 nm (BET) with Purity: 99.8% trace metal basis], was purchased from Sigma-Aldrich Co. Ltd, St. Louis, MO, U.S.A. Particle size and morphology were characterized by a Transmission Electron Microscope (JEOL, JEM-1400 plus Electron Microscope).

The NiO-NPs colloid was prepared as follows: 1. Particles were suspended in normal saline (0.6%) with a final concentration of stock solution of 0.1 mg/ml, 2. sonication for 1 min using a Branson sonifier 450 (Branson Ultrasonics Corp., Danbury, CT, U.S.A.), 3. the suspension was kept on ice for 15 sec, 4. sonication on ice for 10 min at a power of 400 W. Five serially diluted doses were taken from the stock solution (0.01, 0.02, 0.03, 0.04, 0.05, and 0.06 mg/g). All samples were prepared under sterilised conditions.

2.4. Method of treatment

Beetles were injected with serial doses of 0.01, 0.02, 0.03, 0.04, 0.05, and 0.06 mg/g from the NiO-NPs colloid for the determination of the median lethal dose (LD_{50}), which is the dose required to cause 50% mortality. The untreated group received an injection of normal saline. The weight of the adult beetle was approximately 1.87 g.

Beetles were injected while still alive in the ventro-caudal between the 4th and 5th abdominal sclerites. Each beetle was placed on its ventral side and injected with a 1 ml BD hypodermic syringe (27G, "1/ needle) filled with different doses of the NiO-NPs colloid [35] (S2 Fig). The needle was kept horizontally as possible and only its tip was injected to prevent any physical damage of the internal tissues [36]. Mortality was reported daily for 30 days. Cumulative mortality was calculated for each tested dose. The LD_{50} of NiO-NPs was determined by the log-probit model using the LdP LineR software (Ehabsoft (<http://www.ehabsoft.com/ldpline>)) (Table 1, S3 Fig).

Table 1. Dose-response percentages of NiO-NPs in the studied groups.

Dose	Dose 1000 00	Log (Dose1000000)	Treated	Observed mortality response %	Linear mortality response %	Linear probit
0.000001	1	0.0000	20	5.000	2.14291	2.9710
0.01	10000	4.0000	20	35.000	46.6310	4.9154
0.02	20000	4.3010	20	35.000	52.4605	5.0618
0.03	30000	4.4771	20	45.000	55.8561	5.1474
0.04	40000	4.6021	20	50.000	58.2429	5.2081
0.05	50000	4.6990	20	70.000	60.0742	5.2552
0.06	60000	4.7782	20	95.000	61.5507	5.2937

<https://doi.org/10.1371/journal.pone.0255623.t001>

In the mortality test (LD₅₀), the sublethal dose was 0.02 mg/g. The group that received this dose was considered as the treated group (group 2). The tested parameters (enzyme activities, histological analysis, and ultrastructure analysis) were investigated in this group [31].

2.5. Nickel X-ray detection in midgut tissues of *B. polychresta*

The Ni percentage was determined in midgut tissues by using an energy-dispersive X-ray microanalysis (JEOL (JSM-5300) scanning microscope at the Electron Microscope Unit, Faculty of Science, Alexandria University, Egypt). Eight samples of midgut tissues were analysed from each group to estimate the accuracy of the analytical results. SEM EDX software was used to identify the peaks for each metal in the tissue. For each element in the sample, line intensities were measured. It was also measured for the same elements in calibration standards of known composition. A stationary spot (X500) was analysed at random for 110 s.

2.6. Determination of aspartate amino-transferase (AST), alanine amino-transferase (ALT) activities in midgut tissues

Levels of the enzymes AST and ALT in midgut tissues were estimated colorimetrically using a kit purchased from Quimica Clinica Aplicada S.A. Co., Spain, according to the method of Reitman & Frankel (1957) [37].

2.7. Determination of ascorbate levels (APOX) in midgut tissues

Eight samples of the beetles' midgut tissues were homogenized and centrifuged (8000 g, 5 min), and kept on ice. Samples were mixed with 2 M Tris buffer (pH 9.2, 26% v/v) and analysed immediately with reverse-phase HPLC [38]. Ascorbate was separated with a Vydac C-18 column (201 HS, 250 X 4: 6 mm) and guard column, using a mobile phase composed of aqueous ammonium phosphate (20 mM) and EDTA (1.0 mM). The flow rate was 1.0 ml/min (35°C). The peak area was measured with a Shimadzu UV-visible detector (265 nm), and the peak area was integrated with a Shimadzu C-R4A integrator. The identity of the ascorbate peak was determined by analysis of ascorbate standards and confirmed by the treatment of standards and samples with ascorbate oxidase (10 EU (enzyme units)/ml neutralized sample). Peak areas were converted to mU/mg protein injected using an ascorbate standard curve.

2.8. Histological and ultrastructure preparations

The midguts were fixed in 4F₁G in phosphate buffer solution (pH 7.2) at 4°C for 3 h and post-fixed in 2% OsO₄ in the same buffer for 2 h. Samples were washed in the buffer and dehydrated at 4°C through a series of ethanol. Specimens were immersed in an Epon-Araldite mixture in labelled beam capsules. The Ultramicrotome (LKB; Bromma-2088-Ultratome® V, Sweden)

was used for the semithin sections (1 μm thick). Sections were mounted on a glass slide, stained with toluidine blue and examined with a light microscope to determine the orientation and the structural features. Photomicrographs were taken at different magnifications by the Olympus CX31, Leica Ultra Cut R light microscope.

Ultrathin sections (0.06–0.07 μm thick) were cut for transmission electron microscope (TEM) then picked upon 200 mesh naked copper grids. Grids were stained for 30 min with uranyl acetate and 20–30 min with lead citrate (Reynolds 1963). Several magnifications were taken for the electron micrographs. Photographing and scoping the grids were achieved by Jeol 100 CX Tem, at the E.M. Unit, Faculty of Science, Alexandria University, Egypt (JEM-1400 plus; JEOL Ltd., Akishima, Tokyo, Japan)

2.9. Data analysis

The log-probit model, LdP Line^R software (Ehabsoft (<http://www.ehabsoft.com/ldpline>)) was used to estimate the LD₅₀. To estimate mortality, the Kruskal Wallis test for abnormally distributed quantitative variables and comparisons between more than two studied groups was used, and post-hoc (Dunn's multiple comparisons test) for pairwise comparisons. The IBM SPSS software package version 20.0 program (IBM Corp., Armonk, New York, U.S.A.) was used for the analysis of the X-ray and enzymes [39]. The Shapiro-Wilk test was used to prove the normality of the distribution of variables. The Student *t*-test was used to ascertain the difference between the two studied groups for normally distributed quantitative variables [40]. The significance of the results was judged at $P \leq 0.05$.

3. Results

3.1. NiO-NPs characterizations

A Transmission Electron Microscope (TEM) was used to determine the physical characteristics of NiO-NPs. The micrographs showed that the particles were spherical or oval and aggregated together. The size of the particles ranged from 21.79 to 30.35 nm diameter with a mean diameter of 26.27 ± 4.43 nm which was similar to the manufacture's references (<50 nm) (Fig 1).

3.2. Insect mortality

Beetle mortality was calculated from day 1 to day 30 (S1 & S2 Tables). On day 30, it was observed that 13 beetles in groups 1 and 2, 11 beetles in group 3, 10 beetles in group 4, and 6 beetles in group 5 were alive with the injection of 0.01, 0.02, 0.03, 0.04, and 0.05 mg/g respectively, although, total mortality was observed in group 6 (0.06 mg/g) (S1 Table). It was noticed that the 0.04 mg/g dose resulted in 50% mortality and the 0.06 mg/g dose resulted in 100% mortality. A significant difference in the cumulative mortality percentages between the tested groups was observed. (Fig 2, S2 Table). From Table 1, the LD₅₀ was reported at 0.04 mg/g dose, so all the tested parameters were performed in the group that was treated with the sublethal dose of 0.02 mg/g and compared with the untreated group.

3.3. Nickel X-ray detection in the midgut of *B. polychresta*

Ni was detected in the midgut tissues of the treated group by X-ray analysis to determine the metal percentages (Table 2, S4 Fig). Eight elements were detected in the midgut tissue of the untreated group (Na, Al, P, S, K, Ca, Cu, and Zn), whereas, nine elements (Na, Al, P, S, K, Ca, Cu, Zn, and Ni) were detected in the midgut tissues of the NPs treated group, which indicates that Ni was present in the midgut tissues due to the treatment.

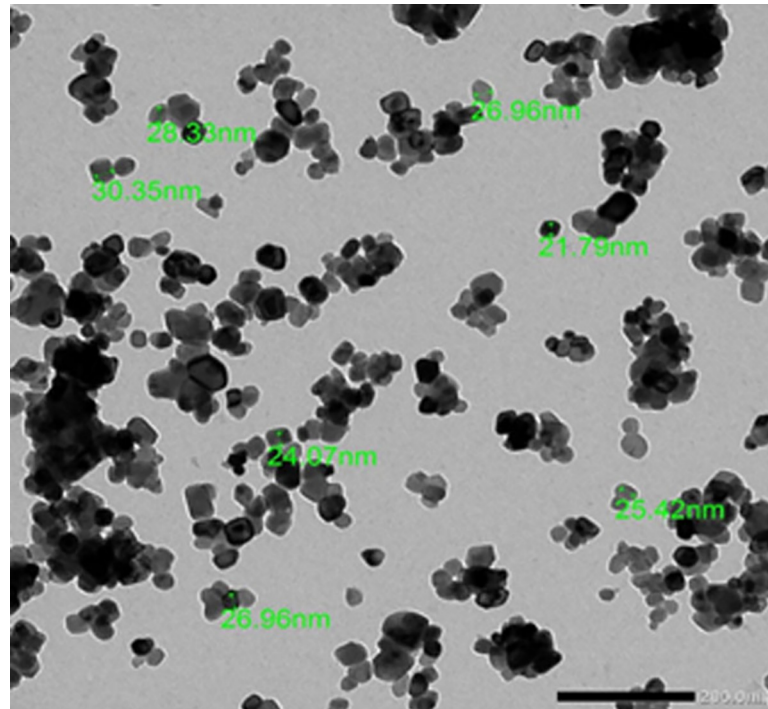


Fig 1. Transmission electron micrograph of NiO-NPs.

<https://doi.org/10.1371/journal.pone.0255623.g001>

3.4. Determination of aspartate amino-transferase (AST), alanine aminotransferase (ALT) and ascorbate peroxidase (APOX) activities in midgut tissues of beetles in the studied groups

In the treated community, AST and ALT enzyme activity levels were significantly higher than in the untreated group in the midgut tissues of beetles (Fig 3A and 3B). However, a substantial reduction in the level of APOX in midgut tissues was found in the treated group as opposed to the untreated group (Fig 3C).

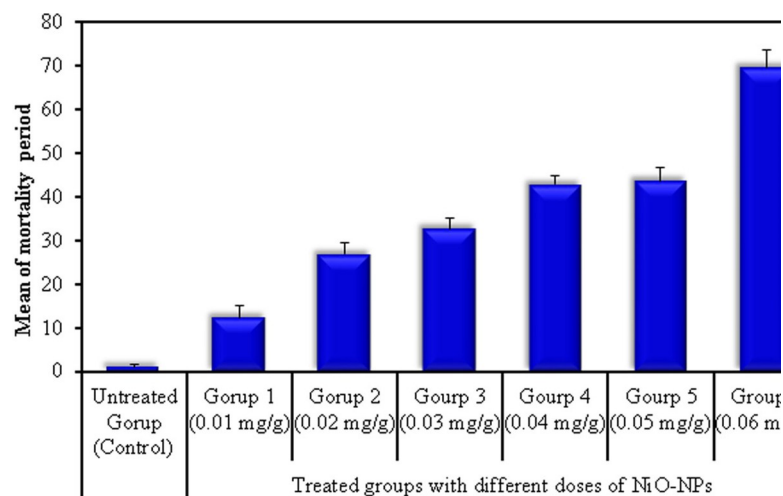


Fig 2. Cumulative mortality percentage in the studied groups during the studied period. The data is presented as a mean \pm SE.

<https://doi.org/10.1371/journal.pone.0255623.g002>

Table 2. Trace metal percentages (%) in midgut tissues of *B. polychresta* of the studied groups.

Metals	Untreated group	Treated group (Group 2)	<i>t</i>	<i>P</i>
Na	5.63 ± 0.48	5.93 ± 1.12	0.246	0.814
Al	10.40 ± 2.10	9.73 ± 3.86	0.154	0.883
P	12.38 ± 2.86	25.20 ± 7.28	1.640	0.178
S	42.65 ± 1.82	29.50 ± 5.25	2.369	0.082
K	4.63 ± 1.33	7.83 ± 3.05	0.963	0.389
Ca	3.78 ± 1.44	2.03 ± 0.53	1.142	0.297
Cu	5.33 ± 0.36	5.55 ± 0.56	0.337	0.748
Zn	4.18 ± 0.36	3.68 ± 0.42	0.904	0.401
Ni	ND	3.45 ± 0.36	–	–

For each metal, the percentage expressed by using minimum–maximum values and mean (n = 8) using Student t-test, *statistically significant at $P \leq 0.05$; ND: not detected.

<https://doi.org/10.1371/journal.pone.0255623.t002>

3.5. The external morphology of the alimentary canal of *B. polychresta*

The alimentary canal of adult *B. polychresta* composed of a short foregut, long midgut, and hindgut (ileum, colon, rectum, and anal canal), which opens outside through the anus between the 8th and 9th sternites (Fig 4A). The anatomical deformity that was observed in the alimentary canals of the treated group was the reduction in the length of the canal, being 7.80 cm in the untreated group (Fig 4A) and 5.60 cm in the treated group (Fig 4B).

3.6. Histological observations of midgut tissues of adult *B. polychresta* in the untreated group

The histological structure of the midgut revealed an epithelium lying on a basement membrane coated by two muscle layers, the circular and the longitudinal muscle fibres (Fig 5A–5C). The epithelium consisted of regenerative cells and digestive cells; columnar cells and goblet cells. Each of these cells had a large nucleus and basophilic cytoplasm (Fig 5A–5C). The regenerative cells appeared singly or in clusters called “nidi”, forming crypts near to the muscle fibres (Fig 5A). In the basal lamina, columnar and goblet cells were observed (Fig 5A–5C). The basal lamina of the epithelium was provided with a striated brush border called microvilli (Fig 5A–5C) that expanded the absorption of the cell surface. The peritrophic membrane appeared visible with multilayer and normal thickness. It was separated from the epithelial cells (Fig 5A).

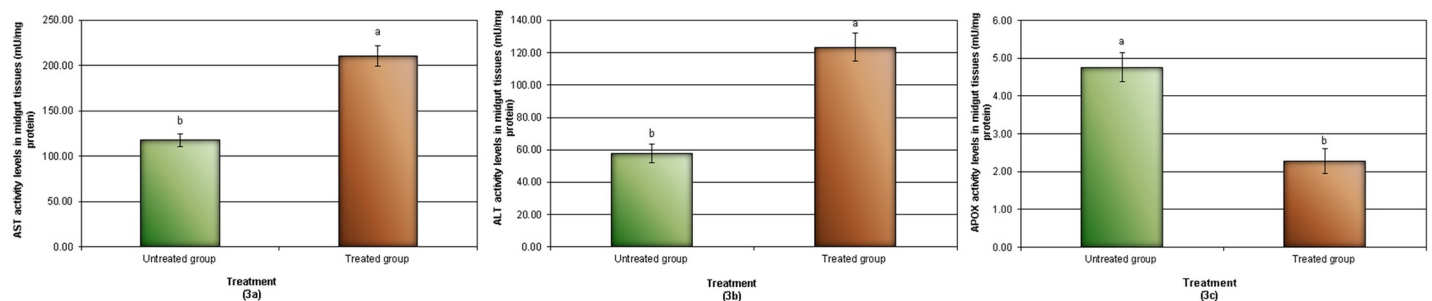


Fig 3. Activities of antioxidant enzymes a: AST, b: ALT, c: APOX in the studied groups. Data are expressed as mean ± SE.

<https://doi.org/10.1371/journal.pone.0255623.g003>

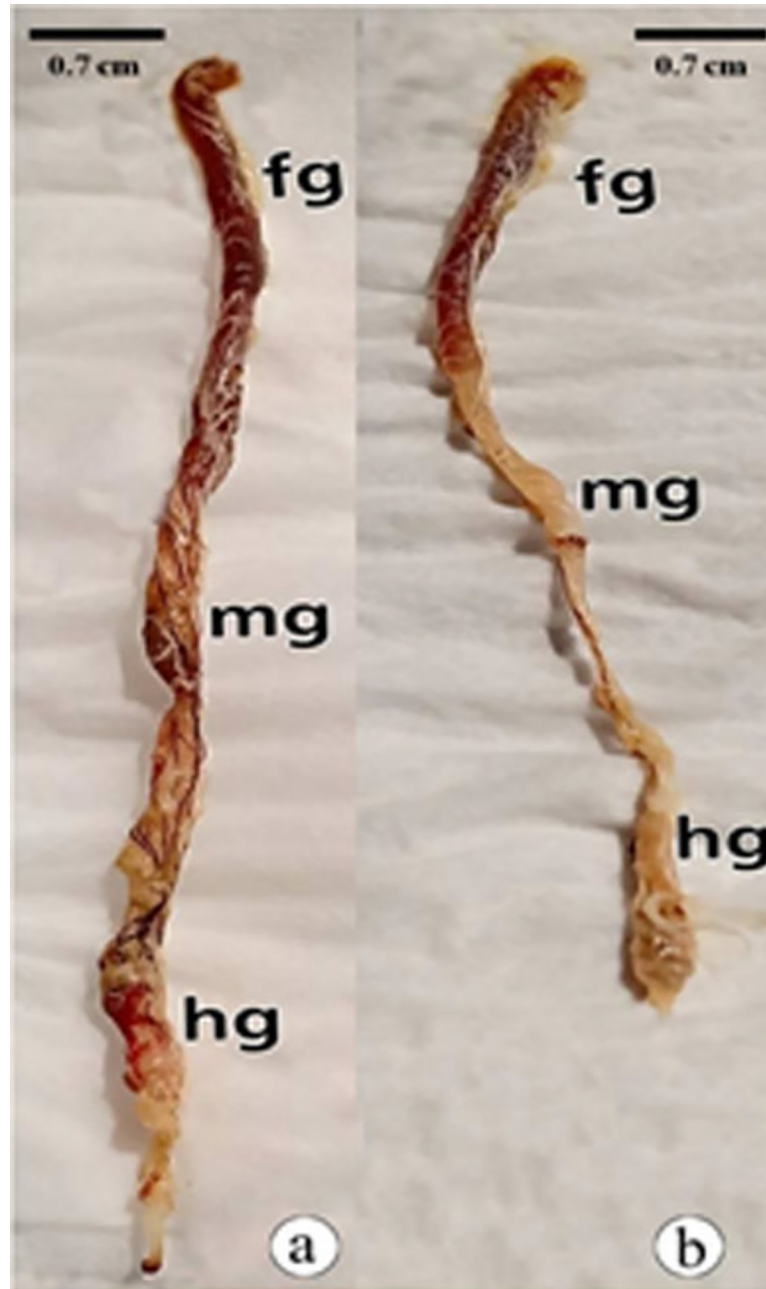


Fig 4. Photograph of the alimentary canal of *B. polychresta*, a: Untreated group b: Treated group. fg: foregut, mg: midgut, hg: hindgut.

<https://doi.org/10.1371/journal.pone.0255623.g004>

3.7. Histological observations of midgut tissues of adult *B. polychresta* in the treated group

Histological alterations in the midgut structure were observed in the treated beetles. Numerous vacuoles, lytic areas, and dense vesicles in the cytoplasm of both cells were observed (Fig 6A–6D). Necrotic regenerative cells with pyknotic nuclei as well as a columnar cell with pyknotic nuclei were distinguished (Fig 6B). Also, disruption of microvilli was observed (Fig 6A–6C).

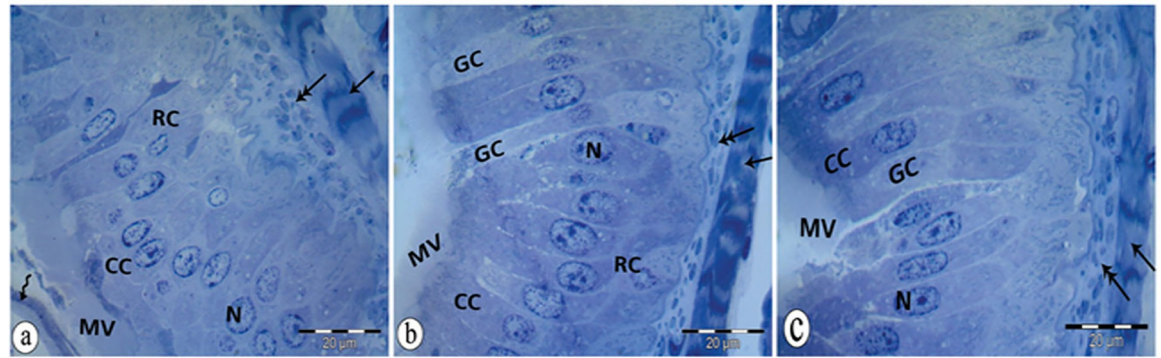


Fig 5. A semithin sections of the midgut epithelium a: circular muscle (arrow), longitudinal muscle (double head arrow), regenerative cell (RC), columnar cell (CC) nucleus (N), microvilli (MV), peritrophic membrane (wavy arrow). b: circular muscle (arrow), longitudinal muscle (double head arrow), regenerative cell (RC), columnar cell (CC), nucleus (N), goblet cell (GC), microvilli (MV). c: circular muscle with light and dark bands (arrow), longitudinal muscle (double head arrow), columnar cell (CC), nucleus (N), goblet cell (GC), microvilli (MV).

<https://doi.org/10.1371/journal.pone.0255623.g005>

The peritrophic membrane was not visible in the micrographs. It might be affected by the NiO-NPs treatment (compare Figs 5A with 6B).

3.8. Ultrastructure observations of midgut tissues of adult *B. polychresta* in the untreated group

Electron micrographs of the midgut of beetles in the untreated group revealed that the regenerative and columnar cells exhibited oval nuclei with patches of heterochromatin and defined nuclear envelopes (Fig 7A and 7D). Cell boundaries and tight junctions were obvious (Fig 7B). Mitochondria, numerous cisterns of the rough endoplasmic reticulum, and free ribosomes were uniformly distributed in the cytoplasm (Fig 7A–7D). Frequent mitochondria in the basal region were noticed (Fig 7C–7F). Unalterable distributed microvilli cover the luminal border (Fig 7D and 7E). Few lysosomes and lipid vacuoles were distinguished (Fig 7C, 7E and 7F).

3.9. Ultrastructure observations of midgut tissues of adult *B. polychresta* in the treated group

Alterations in the midgut cells were observed in the treated beetles. Some nuclei exhibited indentation of the nuclear membranes and pyknotic ones were visible (Fig 8A and 8B). An early apoptotic and achromatic nucleus was detected (Fig 8B). Besides, karyorrhexis was noticed (Fig 8C). The cytoplasm appeared with frequent vacuolations and lytic areas (Fig 8A–8D). Myelin figures were also detected (Fig 8A). Spherical electron-dense particles composed of nanoparticles were distinguished (Fig 8D and 8E). Mitochondria appeared swollen and malformed (Fig 8E). Dilated smooth endoplasmic reticulum (Fig 8C, 8D and 8F), distortion in the brush border of the microvilli (Fig 8E and 8F), and rupture of the cell boundary were observed (Fig 8E).

4. Discussion

Because of the growing interest in using NPs in industry, they are being released into the environment [41] NPs can combine with contaminants due to their high surface to mass ratio, which is a path for ecotoxicity [42]. This combination depends on the physical and chemical properties of the NPs [43]. The liberation of NPs into the soil or water could become a potential lethal factor that induces cellular toxicity [44]. Ni-NPs toxicity is yet to be completely

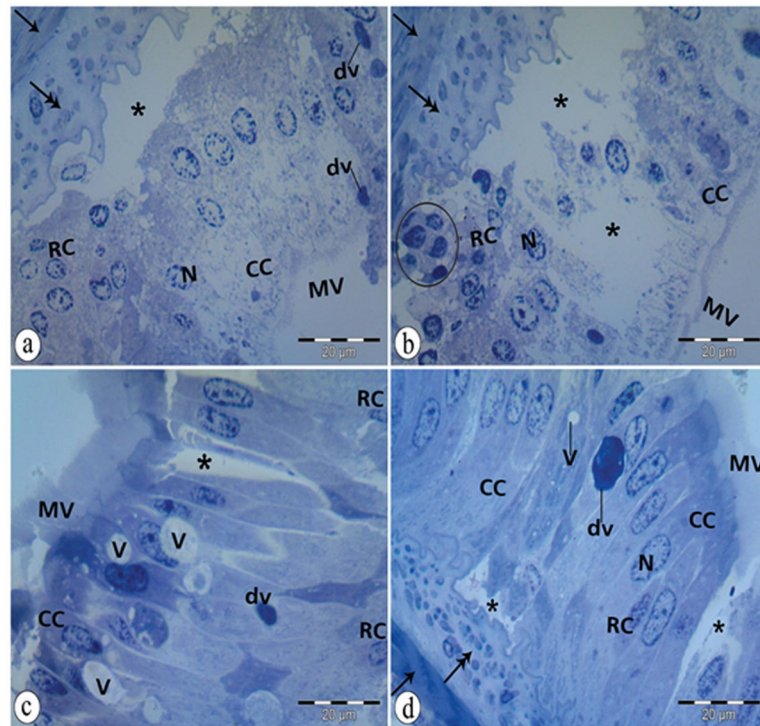


Fig 6. A semithin section of abnormal midgut epithelium. a: lytic cytoplasm (*), regenerative cell (RC) with pale nucleus (N), distorted columnar cell (CC), ruptured microvilli (MV), circular muscle (arrow), longitudinal muscle (double head arrow), dense vesicle (dv). b: massive disruption of the midgut epithelium with lytic cytoplasm (*), distorted microvilli (MV), necrotic regenerative cells (RC) with pyknotic nuclei (circle), columnar cell (CC) with pyknotic nuclei. N: nucleus, double head arrow: longitudinal muscle. c: lytic cytoplasm (*), distortion of microvilli (MV), columnar cell (CC) with a heterochromatic nucleus, regenerative cell (RC), vacuoles (V), dense vesicle (dv). d: lytic cytoplasm (*), microvilli (MV), regenerative cell (RC), columnar cell (CC), nucleus (N), vacuole (V), dense vesicle (dv), circular muscle (arrow), longitudinal muscle (double head arrow).

<https://doi.org/10.1371/journal.pone.0255623.g006>

explained. In the present study, NiO-NPs cytotoxicity has been illustrated in the ground beetle *B. ploycresta* as a biological model. Because beetles can settle in contaminated habitats, they have been successful in biomonitoring programs [10, 17, 32]. Nanoparticles can enter organisms through ingestion or inhalation and are partitioned into tissues where they exert toxic effects [45]. In the current study, a unique route of administration of serial doses of NiO-NPs to the beetles through injection was obtained. This administration route confirms that the chosen doses enter the insect's body. A previous study by Magaye *et al.* [9] reported that the intravenous injection of metallic Ni-NPs in rats caused severe lung and liver injuries.

In the study, Ni was detected by X-ray microanalysis in the midgut tissues of the treated beetles. X-ray microanalysis is a valid tool for illustrating the distribution of metals in biological tissues [46]. The small size, great capacity, and high reactivity of NPs facilitate their transportation to cellular organelles and exert harmful effects, unusual in their micron-sized counterparts [44]. Little data is available in the literature about the toxicity of Ni-NPs in biological tissues. It was reported by Capasso *et al.* [47] that NiO-NPs induced cell cycle retardation in cell lines of human pulmonary epithelials (BEAS-2B and A549). High doses of oral administration of NiO-NPs caused chromosomal aberrations and DNA breaks in Wistar rats [48]. Recent studies show that NiO-NPs have a genotoxic and mutagenic effect in *Drosophila* [6, 49]. Also, Magaye *et al.* [50] stated that Ni-NPs can initiate intracellular oxidative stress, damaging DNA in cells, which is accountable for their genotoxicity.

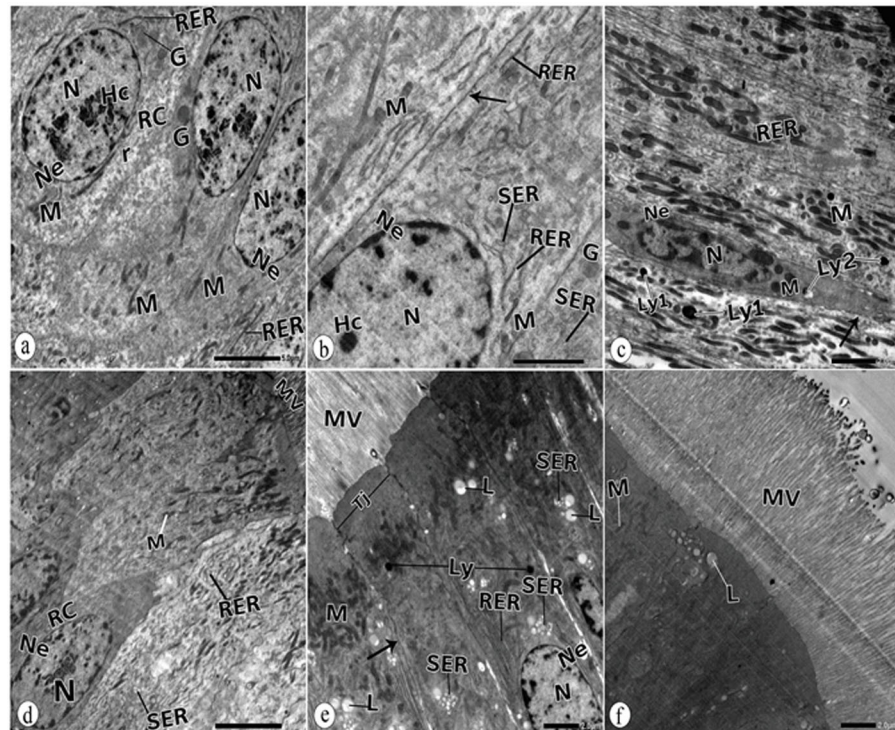


Fig 7. TEM of normal midgut epithelium a: columnar cell (CC) with oval nucleus (N), nuclear envelope (Ne), heterochromatin (Hc), mitochondria (M), rough endoplasmic reticulum (RER), free ribosomes (r). b: nucleus (N), nuclear envelope (Ne), mitochondria (M), heterochromatin (Hc), rough endoplasmic reticulum (RER), smooth endoplasmic reticulum (SER), cell boundary (arrow). c: columnar cell with nucleus (N), nuclear envelope (Ne), mitochondria (M), rough endoplasmic reticulum (RER), primary lysosomes (Ly1), secondary lysosomes (Ly2). d: regenerative cell (RC), nucleus (N), nuclear envelope (Ne), mitochondria (M), rough endoplasmic reticulum (RER), smooth endoplasmic reticulum (SER), microvilli (MV). e: basal nucleus (N), nuclear envelope (Ne), apical mitochondria (M), rough endoplasmic reticulum (RER), smooth endoplasmic reticulum (SER), lysosomes (L), lipid vacuole (L), cell boundary (arrow), tight junction (Tj), microvilli (V), brush border with long microvilli (MV). f: apical mitochondria (M), lipid vacuole (L), brush border with long microvilli (MV).

<https://doi.org/10.1371/journal.pone.0255623.g007>

Toxicological endpoints can be obtained from mortality tests [51]. The mortality test in the present study revealed that the 0.06 mg/g dose resulted in 100% mortality, while the 0.04 mg/g resulted in 50% mortality. Thus, the selected sublethal dose was 0.02 mg/g. Dabour *et al.* [31] reported the mortality of honey bee workers (*Apis mellifera*) due to exposure to sublethal concentrations of PbO and CdO NPs (0.65 mg/ml, and 0.01 mg/ml respectively), which is hardly comparable to the present work.

In the present study, a disturbance in the enzyme activities (significant elevation in AST, ALT and significant inhibition of APOX) was reported in the treated group compared with the untreated one. The elevation in transaminase activities might be required to shift amino acids to the tricyclic acid cycle, so they can be used as fuel molecules to produce additional energy in the stressed organism [52]. Transaminase activities were remoulded during various pathological conditions [53, 54]. This insinuates that injected NiO-NPs may generate toxic reactions. Upadhyay [52] reported that the elevation in the activities of AST and ALT designates tissue damage. After fourteen days of intravenous injection, Magaye *et al.* [9] discovered that Ni nanoparticles significantly increase alkaline phosphatase (ALP) and significantly decrease alanine aminotransferase (ALT) in the liver of rats, while no significant difference in aspartate aminotransferase (AST) is observed. Stohs *et al.* [55] stated that the molecular action of heavy

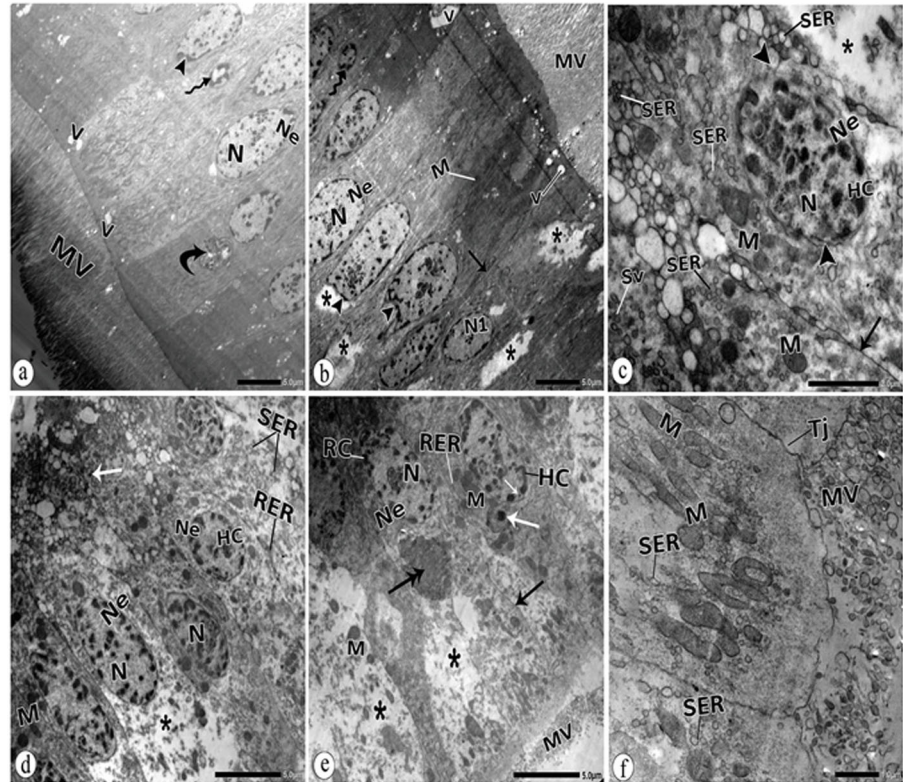


Fig 8. TEM of the treated midgut epithelium a: nucleus (N) with irregular nuclear envelope Ne (head arrow), pyknotic nucleus (wavy arrow), vacuoles (V), myelin figure (curved arrow), microvilli (MV). b: lytic cytoplasm (*), intended nuclear envelopes (head arrow), early apoptotic nucleus (wavy arrow), achromatic nucleus (N1), vacuoles (V), microvilli (MV). N: nucleus, Ne: nuclear envelope. c: lytic cytoplasm (*) heterochromatic nucleus (N), heterochromatin (Hc), karyorrhexis (head arrow) at the nuclear envelope (Ne), swollen mitochondria (M), dilated smooth endoplasmic reticulum (SER), secretory vesicle (Sv). d: lytic cytoplasm (*), nucleus (N), heterochromatin (Hc), dilated smooth endoplasmic reticulum (SER), rough endoplasmic reticulum (RER). e: lytic cytoplasm (*), electron-dense particles (white arrow), heterochromatin (Hc), irregular nuclear envelope Ne (head arrow), swollen mitochondria (M), aggregation of malformed mitochondria (double head arrow), ruptured cell boundary (arrow), distorted microvilli (MV). f: brush border with distorted microvilli (MV), swollen mitochondria (M), dilated smooth endoplasmic reticulum (SER), tight junction (Tj).

<https://doi.org/10.1371/journal.pone.0255623.g008>

metals provokes ROS, which ushers in cell toxicity. Ni-NPs were found to induce oxidative stress evinced by the generation of reactive oxygen species (ROS), which suggests that the Ni-NPs are capable of inducing genotoxic effects [6, 56]. Some research has proved that diverse kinds of nanoparticles can trigger oxidative stress in arthropod tissues [57, 58]. Rai *et al.* (2014) [59] stated that the penetration of the nanoparticles through the exoskeleton can induce toxicity. Nanomaterials bind to sulphur from proteins or to phosphorus from DNA in the intracellular space, leading to denaturation of enzymes and organelles [60]. Nel *et al.* (2006) [61] and Wise *et al.* [62] stated that oxidative stress and ROS generation are possible mechanisms of cytotoxicity related to NP exposure. Moreover, it has been suggested that NPs induce oxidative stress that leads to DNA damage and apoptosis [63]. Siddiqui *et al.* (2012) [64] found that NiO-NPs increased apoptosis in MCF-7 and HEp-2 cells *in vitro*. The inhibition of APOX activities in the study might be an outcome of structural alterations of proteins, damage, and finally deactivation of the enzymes [65–67]. APOX catalysed the reduction of H₂O₂ using ascorbate as a reducing agent. Therefore, the activity of the enzyme can be limited by the

prevalence of reduced ascorbate. The production of reduced ascorbate is sustained under favourable conditions, although the process could be disrupted under stressed conditions [67]. Lijun *et al.* 2005 [68] stated that antioxidant enzymes activities, such as APOX are changed at high Cd concentrations as an outcome of protein alteration. Due to the shape and surface characteristics charge of NPs, they can bind to the proteins and generate adverse biological outcomes such as protein unfolding, thiol crosslinking, fibrillation, and loss of enzymatic activity [69]. Also, cytotoxicity will occur from the release of toxic ions because the thermodynamic properties of materials favour particle cessation in a biological medium [69]. However, in the light of these conclusions, NiO-NPs might have a role in enzymatic activity alterations and protein denaturation.

The histological observations of the midgut of the NiO-NPs treated group showed acute and irreversible pathological anomalies. Abdollahi *et al.* [70] stated that the toxicity of xenobiotics is related to the production of free radicals, which are implicated in physiological and histological pathology. A disorganisation of the microvilli was noticed in our preparations that may be a consequence of the rupture of the peritrophic membrane. In the midgut of insects, the peritrophic membrane envelopes the food [71]. Abu El-Saad *et al.* [72] reported that the midgut epithelium is the main object of toxins as it is considered the first barrier against the intoxication of the organism. Other observed alterations in the current study included disruption of the epithelial cells as observed by Rawi *et al.* [73], and the appearance of vacuoles as reported by Younes *et al.* [74], Adel *et al.* [75] and Osman *et al.* [34]. These pathological alterations in the cells may affect the normal physiology of insects [76]. It was cited that zinc oxide nanoparticles led to several morphological and histological abnormalities in *Ae. aegypti* third instar larvae (exposed to LC₅₀ of 1.57 mg/l for 24 h), including shrinkage in the abdominal region, thorax shape changes, and midgut damage [77].

Several types of research have postulated the histopathological effects of metal/metalloids on the insect's gut. Zhang *et al.* [29] observed stretching of the cellular axis, an increase of the cellular volume, cytoplasmic vacuolations, and an inhibition of basophilic secretions towards the lumen in the midgut of *Blattella germanica* after treatment with heavy metals (Hg, Pb and Cr). Al-Dhafar & Sharaby [78] observed degeneration, vacuolation, and shrinkage of some epithelial and goblet cells in the midgut of the larvae of *Rhynchophorus ferrugineus* after treatment with ZnSO₄. Cid *et al.* [79] observed histological anomalies (vacuolisation and thickening) in digestive gland cells of freshwater bivalves (*Corbicula fluminea*) after exposure to various concentrations of nanodiamonds (NDs, 0.01, 0.1, 1, and 10 mg/l) for 14 days.

Krishnan *et al.* [80] attributed the damage to the gut to the ROS effect. An excess of ROS reduces nutrient absorption and damages midgut cells, resulting in a nonfunctional digestive system. According to Krishnan and Kodrik [81], ROS can oxidise PUFA in the cell membranes and inhibit its function. Dabour *et al.* postulated the adverse consequences of food administration of sublethal concentrations of CdO and PbO NPs on the cellular and subcellular structures of the midgut of honey bee workers (*Apis mellifera*). They found that CdO and PbO NPs marked out various histological anomalies in the NPs fed group compared with controls. One of the histopathological alterations in the midgut tissues of the NiO-NPs treated group in the current study is the rupture of PM. These results are consistent with those reported by Dabour *et al.* [31] who noticed the destruction of PM after food administration of sublethal concentrations of CdO and PbO to honey bee workers (*Apis mellifera*). The PM serves as a protective barrier against chemical, physical and microbial food components [82, 83]. Therefore, any alteration in its structure leads to deleterious effects on the midgut tissues of insects.

Ultrastructure deformities in the NiO-NPs treated group involve chromatin clumping and the presence of pyknotic nuclei, which suggests less efficient transcription and subsequently result in the decrease in metabolic activity [84]. This also indicates that cells are in an advanced

cell death process [85, 86]. The irregularity of the nuclear envelopes and karyorrhexis indicate a pathway of cell death [87, 88]. Some authors attributed apoptosis to metal accumulation [89, 90], which is in agreement with our results. Research has proven the relation between exposure to metals and the prevalence of apoptosis [91, 92]. The vacuolated areas in the cytoplasm may be ascribed to the action of lysosomal hydrolase or the breakage of the mitochondria [93] and sometimes may be due to the enhanced endocytotic activity as described by Cavados *et al.* [94].

Nanoparticles are frequently distinguished from lysosomes upon internalisation, and numerous nanomaterials have been related to lysosomal impairments [95]. It has been confirmed that lysosomal destabilisation activates mitochondrial apoptosis [96, 97].

The study revealed the presence of electron-dense particles in the midgut tissues due to NiO-NPs accumulations as a detoxification mechanism [98, 99]. Our results follow Polidori *et al.* (2018) [93], who detected metal precipitation in spherites in the midgut of paper wasps (*Polistes dominula*) collected from urban environments. Also, a similar observation was noticed by Pigino *et al.* [100], who reported that a large number of electron-dense granules, composed of a variety of heavy metals, were accumulated in the epithelium of the midgut ventriculus of the mite *Xenillus tegeocranus* from a deserted mining and smelting area. Karpeta-Kaczmarek *et al.* [101] reported that the epithelial cells of midgut and hindgut of *Acheta domesticus* (Orthoptera, Gryllidae) were damaged at high concentrations of nanodiamonds (NDs) and autophagy was activated. The hydrophobic nature of NPs allows them to cross the cell membranes [102] and then they may act as centres of oxidative damage inside the cell [103].

Disruption of microvilli is one of our major findings in this study since it is the first site facing and interacting with pollutants [93]. Some changes in the cytoplasmic organelles were distinguished in our electron micrographs, such as lysis of mitochondrial matrices, dilated rough and smooth endoplasmic reticulum, and the presence of myelin figures. It was found that heavy metals distort cytoplasmic membranes [10, 17]. Mitochondrial alteration is a reflection of the deregulation of mitochondrial membrane transport [104]. Toxins cause damage to mitochondrial membranes and cristae, as discovered by Braeckman *et al.* [105] in insects' intoxicated cells. Moreover, the swelling of the mitochondria reflects the entry of water and/or solutes into the mitochondrial matrix [106]. Belyaeva *et al.* [107] deduced that mitochondria are an important target for the toxic effects of metals and their oxide NPs.

The interference of heavy metals with proper processing in the ER causes its dilation and activates the ER stress response [108]. The proliferation of myelin figures in our preparations has been interpreted as a symptom of intoxication triggered by NiO-NPs that implies an adaptive mechanism in response to the high degradation of cellular organelles [109]. These ultrastructure alterations represent the major features of both cell necrosis and apoptosis [110, 111]. In accordance with our results, Dabour *et al.* [31] observed ultrastructure anomalies in the midgut cells of workers of honey bees (*Apis mellifera*) treated with CdO and PbO-NPs.

The present results are considered the first record to present the physiological and histological alterations induced by NiO-NPs in the ground beetle *B. polychresta*. However, the processes behind NiO-NPs' toxicity remain unknown. Additionally, the effect of nanoscale dimensions, form, and charge on the different possible mechanisms of action will be examined in more detail in our upcoming work.

5. Conclusion

The findings of the current study will guide researchers to identify the impact of the sublethal dose of NiO-NPs on biological tissues. It could be concluded that particles, which are less than

50 nm, are capable of entering cells and attaching to macromolecules, leading to DNA damage. Thus, precautions should be taken when dealing with minute particles. The mechanisms responsible for the toxicity of NiO-NPs still need to be investigated. Also, the impact of nano size, shape, and charge on the various potential mechanisms of action must be elucidated. Lastly, further efforts are still necessary to validate the proposed metal oxide nanoparticles in field conditions, monitoring at the same time their stability, fate in the environment, and sub-lethal effects on non-target organisms.

Supporting information

S1 Fig. Photograph of photograph of *Blaps polycresta*.

(DOCX)

S2 Fig. A photograph shows the route of administration of NiO-NPs ventro-caudal through the arthrodial membrane between the 4th and 5th abdominal sclerites.

(DOCX)

S3 Fig. Linear dose-mortality response percentages of NiO-NPs in the studied groups.

(DOCX)

S4 Fig. Energy-dispersive X-ray spectra reveal the qualitative elemental composition as measured in counts per second in the midgut tissues of *B. polychresta* of the studied groups. Horizontal scale, X-ray energy; vertical scale, X-ray counts.

(DOCX)

S1 Table. Mortality counts of beetles in the untreated and NiO-NPs treated groups for 30 days.

(DOCX)

S2 Table. Mean \pm SE of the cumulative mortality percentages in the studied groups.

(DOCX)

S3 Table. Enzyme activities in midgut tissues (mU/mg protein) of *B. polychresta* from the studied groups.

(DOCX)

Acknowledgments

The authors are thankful to the Zoology Department and Electron microscope unit, Faculty of Science, Alexandria University.

Author Contributions

Conceptualization: Saeed El-Ashram, Awatef M. Ali, Salah E. Osman, Shujian Huang, Amal M. Shouman, Dalia A. Kheirallah.

Formal analysis: Awatef M. Ali, Salah E. Osman, Amal M. Shouman, Dalia A. Kheirallah.

Methodology: Awatef M. Ali, Salah E. Osman, Dalia A. Kheirallah.

Writing – original draft: Awatef M. Ali, Salah E. Osman, Amal M. Shouman, Dalia A. Kheirallah.

Writing – review & editing: Saeed El-Ashram, Awatef M. Ali, Salah E. Osman, Amal M. Shouman, Dalia A. Kheirallah.

References

1. Sezer Tuncsoy B, Tuncsoy M, Gomes T, Sousa V, Teixeira MR, Bebianno MJ, et al. Effects of Copper Oxide Nanoparticles on Tissue Accumulation and Antioxidant Enzymes of *Galleria mellonella* L. *Bull Environ Contam Toxicol*. 2019; 102(3):341–6. <https://doi.org/10.1007/s00128-018-2529-8> PMID: 30600390
2. Rana S, Bajaj A, Mout R, Rotello VM. Monolayer coated gold nanoparticles for delivery applications. *Adv Drug Deliv Rev*. 2012; 64(2):200–16. <https://doi.org/10.1016/j.addr.2011.08.006> PMID: 21925556
3. Wu Q-S, Liu J-W, Wang G-S, Chen S-F, Yu S-H. A surfactant-free route to synthesize BaxSr1-xTiO3 nanoparticles at room temperature, their dielectric and microwave absorption properties. *Sci China Material*. 2016; 59(8):609–17. <https://doi.org/10.1007/s40843-016-5072-5>.
4. Dorne JL, Kass GE, Bordajandi LR, Amzal B, Bertelsen U, Castoldi AF, et al. Human risk assessment of heavy metals: principles and applications. *Met Ions Life Sci*. 2011; 8:27–60. <https://doi.org/10.1039/9781849732116-00027>. PMID: 21473375
5. Panacek A, Prucek R, Safarova D, Dittrich M, Richtrova J, Benickova K, et al. Acute and chronic toxicity effects of silver nanoparticles (NPs) on *Drosophila melanogaster*. *Environ Sci Technol*. 2011; 45(11):4974–9. <https://doi.org/10.1021/es104216b> PMID: 21553866
6. Carmona ER, García-Rodríguez A, Marcos R. Genotoxicity of Copper and Nickel Nanoparticles in Somatic Cells of *Drosophila melanogaster*. *J Toxicol*. 2018; 2018:7278036. <https://doi.org/10.1155/2018/7278036> PMID: 30111998
7. Magaye R, Zhao J, Bowman L, Ding M. Genotoxicity and carcinogenicity of cobalt-, nickel- and copper-based nanoparticles. *Exp Ther Med*. 2012; 4(4):551–61. <https://doi.org/10.3892/etm.2012.656> PMID: 23170105
8. Kong L, Tang M, Zhang T, Wang D, Hu K, Lu W, et al. Nickel nanoparticles exposure and reproductive toxicity in healthy adult rats. *Int J Mol Sci*. 2014; 15(11):21253–69. <https://doi.org/10.3390/ijms151121253> PMID: 25407529
9. Magaye RR, Yue X, Zou B, Shi H, Yu H, Liu K, et al. Acute toxicity of nickel nanoparticles in rats after intravenous injection. *Int J Nanomedicine*. 2014; 9:1393–402. <https://doi.org/10.2147/IJN.S56212> PMID: 24648736
10. Kheirallah D, El-M Z, El-Gendy D. Impact of Cement Dust on the Testis of *Tachyderma hispida* (Forsk., 1775) (Coleoptera: Tenebrionidae), Inhabiting Mariout Region (Alexandria, Egypt). *J Entomol*. 2016; 13:55–71. <https://doi.org/10.3923/je.2016.55.71>.
11. Mirzoyan Z, Sollazzo M, Allocca M, Valenza AM, Grifoni D, Bellosta P. *Drosophila melanogaster*: A Model Organism to Study Cancer. *Front Genet*. 2019; 10:51. <https://doi.org/10.3389/fgene.2019.00051> PMID: 30881374
12. Herranz H, Eichenlaub T, Cohen SM. Cancer in *Drosophila*: Imaginal Discs as a Model for Epithelial Tumor Formation. *Curr Top Dev Biol*. 2016; 116:181–99. <https://doi.org/10.1016/bs.ctdb.2015.11.037> PMID: 26970620
13. Chen F, Lu J, Zhang M, Wan K, Liu D. Mulberry nutrient management for silk production in Hubei Province of China. *J Plant Nutr Soil Sci*. 2009; 172(2):245–53. <https://doi.org/https://doi.org/10.1002/jpln.200800093>.
14. Fattorini S, Santoro R, Maurizi E, Acosta AT, Di Giulio A. Environmental tuning of an insect ensemble: the tenebrionid beetles inhabiting a Mediterranean coastal dune zonation. *C R Biol*. 2012; 335(10–11):708–11. <https://doi.org/10.1016/j.crv.2012.09.009> PMID: 23199639
15. Bhargava V. Assessing the potential role of Coleoptera (Insecta) as bioindicators in Simbalbara Wildlife Sanctuary, Himachal Pradesh. PhD Thesis. Dehradun: Wildlife Institute of India; 2009.
16. Wise DH. Seasonal and Yearly Patterns in the Densities of Darkling Beetles (Coleoptera: Tenebrionidae) in a Montane Community. *Environ Entomol*. 1981; 10(3):350–8. <https://doi.org/10.1093/ee/10.3.350>.
17. Shonouda M, Osman W. Ultrastructural alterations in sperm formation of the beetle, *Blaps polycresta* (Coleoptera: Tenebrionidae) as a biomonitor of heavy metal soil pollution. *Environ Sci Pollut Res Int*. 2018; 25(8):7896–906. <https://doi.org/10.1007/s11356-017-1172-y> PMID: 29299863
18. Asharani PV, Lian Wu Y, Gong Z, Valiyaveetil S. Toxicity of silver nanoparticles in zebrafish models. *Nanotechnology*. 2008; 19(25):255102. <https://doi.org/10.1088/0957-4484/19/25/255102> PMID: 21828644
19. Peterson RT, Fishman MC. Discovery and use of small molecules for probing biological processes in zebrafish. *Methods Cell Biol*. 2004; 76:569–91. [https://doi.org/10.1016/s0091-679x\(04\)76026-4](https://doi.org/10.1016/s0091-679x(04)76026-4) PMID: 15602893
20. Migula P, Laszczyca P, Augustyniak M, Wilczek G, Rozpedek K, Kafel A, et al. Antioxidative defence enzymes in beetles from a metal pollution gradient. *Biol Bratisl*. 2004; 59(5):645–54

21. Crane M, Sildanchandra W, Kheir R, Callaghan A. Relationship between biomarker activity and developmental endpoints in *Chironomus riparius* Meigen exposed to an organophosphate insecticide. *Ecotoxicol Environ Saf.* 2002; 53(3):361–9. [https://doi.org/10.1016/s0147-6513\(02\)00038-6](https://doi.org/10.1016/s0147-6513(02)00038-6) PMID: 12485579
22. Fontanetti C, Nogarol L, de Souza R, Perez D, Maziviero G. Bioindicators and Biomarkers in the Assessment of Soil Toxicity. In: Pascucci S, (ed). *Soil Contamination*. London: IntechOpen; 2011. 143–68.
23. El-Moaty ZA, Kheirallah DA, Elgendy DA. Impact of cement dust on some biological parameters of *Trachyderma hispida* (Coleoptera: Tenebrionidae) inhabiting the vicinity of a cement factory, Mariout region, Alexandria, Egypt. *J Entomol Zool Studies.* 2016; 4(5):797–805
24. Azmi MA, Naqvi SNH, Khan MF, Akhtar K, Khan FY. Comparative toxicological studies of RB-a (Neem Extract) and Coopex (Permethrin+ Bioallethrin) against *Sitophilus oryzae* with reference to their effects on oxygen consumption and GOT, GPT activity. *Turk J Zool.* 1998; 22(4):307–10
25. Feig DI, Sowers LC, Loeb LA. Reverse chemical mutagenesis: identification of the mutagenic lesions resulting from reactive oxygen species-mediated damage to DNA. *Proc Natl Acad Sci U S A.* 1994; 91(14):6609–13. <https://doi.org/10.1073/pnas.91.14.6609> PMID: 7517554
26. Asada K. Ascorbate peroxidase—a hydrogen peroxide-scavenging enzyme in plants. *Physiologia Plantarum.* 1992; 85(2):235–41. <https://doi.org/10.1111/j.1399-3054.1992.tb04728.x>.
27. Mathews MC, Summers CB, Felton GW. Ascorbate peroxidase: A novel antioxidant enzyme in insects. *Arch Insect Biochem Physiol.* 1997; 34(1):57–68. [https://doi.org/10.1002/\(SICI\)1520-6327\(1997\)34:1<57::AID-ARCH5>3.0.CO;2-T](https://doi.org/10.1002/(SICI)1520-6327(1997)34:1<57::AID-ARCH5>3.0.CO;2-T).
28. Higes M, Meana A, Bartolomé C, Botías C, Martín-Hernández R. *Nosema ceranae* (Microsporidia), a controversial 21st century honey bee pathogen. *Environ Microbiol Rep.* 2013; 5(1):17–29. <https://doi.org/10.1111/1758-2229.12024> PMID: 23757127
29. Zhang Y, Lambiasi S, Fasola M, Gandini C, Grigolo A, Laudani U. Mortality and tissue damage by heavy metal contamination in the German cockroach, *Blattella germanica* (Blattaria, Blattellidae). *Italian J Zool.* 2001; 68(2):137–45. <https://doi.org/10.1080/11250000109356398>.
30. Catae AF, Roat TC, De Oliveira RA, Nocelli RC, Malaspina O. Cytotoxic effects of thiamethoxam in the midgut and malpighian tubules of Africanized *Apis mellifera* (Hymenoptera: Apidae). *Microsc Res Tech.* 2014; 77(4):274–81. <https://doi.org/10.1002/jemt.22339> PMID: 24470251
31. Dabour K, Al Naggar Y, Masry S, Naiem E, Giesy JP. Cellular alterations in midgut cells of honey bee workers (*Apis mellifera* L.) exposed to sublethal concentrations of CdO or PbO nanoparticles or their binary mixture. *Sci Total Environ.* 2019; 651(Pt 1):1356–67. <https://doi.org/10.1016/j.scitotenv.2018.09.311> PMID: 30360267
32. Kheirallah D, El-Samad L. Histological and ultrastructure alterations in the midgut of *Blaps polycresta* and *Trachyderma hispida* (Coleoptera: Tenebrionidae) induced by heavy metals pollution. *Asian J Biol Sci.* 2019; 12(4):637. <https://doi.org/10.3923/ajbs.2019.637.647>.
33. Condamine FL, Soldati L, Rasplus J-Y, Kergoat GJ. New insights on systematics and phylogenetics of Mediterranean *Blaps* species (Coleoptera: Tenebrionidae: Blaptini), assessed through morphology and dense taxon sampling. *System Entomol.* 2011; 36(2):340–61. <https://doi.org/10.1111/j.1365-3113.2010.00567.x>.
34. Osman W, El-Samad LM, Mokhamer el H, El-Touhamy A, Shonouda M. Ecological, morphological, and histological studies on *Blaps polycresta* (Coleoptera: Tenebrionidae) as biomonitors of cadmium soil pollution. *Environ Sci Pollut Res Int.* 2015; 22(18):14104–15. <https://doi.org/10.1007/s11356-015-4606-4> PMID: 25963070
35. Leonard C, Söderhäll K, Ratcliffe NA. Studies on prophenoloxidase and protease activity of *Blaberus craniifer* haemocytes. *Insect Biochem.* 1985; 15(6):803–10. [https://doi.org/10.1016/0020-1790\(85\)90109-X](https://doi.org/10.1016/0020-1790(85)90109-X).
36. de Viedma M, Nelson M. Notes on Insect Injection, Anesthetization, and Bleeding. *Great Lakes Entomol.* 2017; 10(4):12
37. Reitman S, Frankel S. A colorimetric method for the determination of serum glutamic oxalacetic and glutamic pyruvic transaminases. *Am J Clin Pathol.* 1957; 28(1):56–63. <https://doi.org/10.1093/ajcp/28.1.56> PMID: 13458125
38. Levine M, Wang Y, Rumsey SC. Analysis of ascorbic acid and dehydroascorbic acid in biological samples. *Methods Enzymol.* 1999; 299:65–76. [https://doi.org/10.1016/s0076-6879\(99\)99009-2](https://doi.org/10.1016/s0076-6879(99)99009-2) PMID: 9916197
39. Kirkpatrick L, Feeney B. *A Simple Guide to IBM SPSS Statistics for Version 20.0*. Wadsworth: Cengage Learning; 2013.

40. Sokal R, Rohlf F. *Biometry: the Principles and Practice of Statistics in Biological Research*. 2nd ed. New York: W.H. Freeman; 1981.
41. Ripp S, Henry T. *Biotechnology and Nanotechnology Risk Assessment: Minding and Managing the Potential Threats around US: ACS Symposium Series*. Washington: American Chemical Society; 2011.
42. Golobič M, Jemec A, Drobne D, Romih T, Kasemets K, Kahru A. Upon exposure to Cu nanoparticles, accumulation of copper in the isopod *Porcellio scaber* is due to the dissolved Cu ions inside the digestive tract. *Environ Sci Technol*. 2012; 46(21):12112–9. <https://doi.org/10.1021/es3022182> PMID: 23046103
43. Santra S, Zhang P, Wang K, Tapeç R, Tan W. Conjugation of biomolecules with luminophore-doped silica nanoparticles for photostable biomarkers. *Anal Chem*. 2001; 73(20):4988–93. <https://doi.org/10.1021/ac010406+> PMID: 11681477
44. Khan I, Saeed K, Khan I. Nanoparticles: properties, applications and toxicities. *Arab JChem*. 2017; 12(7):908–31. <https://doi.org/10.1016/j.arabjc.2017.05.011>.
45. Navarro E, Piccapietra F, Wagner B, Marconi F, Kaegi R, Odzak N, et al. Toxicity of silver nanoparticles to *Chlamydomonas reinhardtii*. *Environ Sci Technol*. 2008; 42(23):8959–64. <https://doi.org/10.1021/es801785m> PMID: 19192825
46. Kheirallah DA, El-Samad LM. Isoenzymes and protein polymorphism in *Blaps polycresta* and *Trachyderma hispida* (Forsskål, 1775) (Coleoptera: Tenebrionidae) as biomarkers for ceramic industrial pollution. *Environ Monit Assess*. 2019; 191(6):372. <https://doi.org/10.1007/s10661-019-7517-x> PMID: 31101990
47. Capasso L, Camatini M, Gualtieri M. Nickel oxide nanoparticles induce inflammation and genotoxic effect in lung epithelial cells. *Toxicol Lett*. 2014; 226(1):28–34. <https://doi.org/10.1016/j.toxlet.2014.01.040> PMID: 24503009
48. Dumala N, Mangalampalli B, Chinde S, Kumari SI, Mahoob M, Rahman MF, et al. Genotoxicity study of nickel oxide nanoparticles in female Wistar rats after acute oral exposure. *Mutagenesis*. 2017; 32(4):417–27. <https://doi.org/10.1093/mutage/gex007> PMID: 28387869
49. De Carli RF, Chaves DDS, Cardozo TR, de Souza AP, Seeber A, Flores WH, et al. Evaluation of the genotoxic properties of nickel oxide nanoparticles in vitro and in vivo. *Mutat Res Genet Toxicol Environ Mutagen*. 2018; 836(Pt B):47–53. <https://doi.org/10.1016/j.mrgentox.2018.06.003> PMID: 30442345
50. Magaye R, Gu Y, Wang Y, Su H, Zhou Q, Mao G, et al. In vitro and in vivo evaluation of the toxicities induced by metallic nickel nano and fine particles. *J Mol Histol*. 2016; 47(3):273–86. <https://doi.org/10.1007/s10735-016-9671-6> PMID: 27010930
51. Swidan MH, Kheirallah DA, Osman SEI, Nour FE. Impact of Certain Natural Insecticides on the Morphological and Biochemical Characteristics of Khapra beetle, *Trogoderma granarium* Everts. *Int J Zool Invest*. 2016; 2(1):147–66
52. Upadhyay R. *Capparidaceae Induced Toxicity, Biochemical and Enzymatic Alterations in Rhizophortheadominica* (Fabr.) (Coleoptera: Bostrichidae). *World J Zool*. 2013; 8(3):256–66. <https://doi.org/10.5829/idosi.wjz.2013.8.3.73227>.
53. Etebari K, Mirhoseini SZ, Matindoost L. A study on interspecific biodiversity of eight groups of silkworm (*Bombyx mori*) by biochemical markers. *Insect Sci*. 2005; 12(2):87–94. <https://doi.org/10.1111/j.1744-7917.2005.00010.x>.
54. Içen E, Armutçu F, Büyükgüzel K, Gürel A. Biochemical stress indicators of greater wax moth exposure to organophosphorus insecticides. *J Econ Entomol*. 2005; 98(2):358–66. <https://doi.org/10.1111/j.15889724> PMID: 15889724
55. Stohs SJ, Bagchi D, Hassoun E, Bagchi M. Oxidative mechanisms in the toxicity of chromium and cadmium ions. *J Environ Pathol Toxicol Oncol*. 2000; 19(3):201–13. <https://doi.org/10.1615/JEnvironPatholToxicolOncol.v20.i2.10> PMID: 10983887
56. Alarifi S, Ali D, Alakhtani S, Al Suhaibani ES, Al-Qahtani AA. Reactive oxygen species-mediated DNA damage and apoptosis in human skin epidermal cells after exposure to nickel nanoparticles. *Biol Trace Elem Res*. 2014; 157(1):84–93. <https://doi.org/10.1007/s12011-013-9871-9> PMID: 24307203
57. Mao H, Wang DH, Yang WX. The involvement of metallothionein in the development of aquatic invertebrate. *Aquat Toxicol*. 2012; 110–111:208–13. <https://doi.org/10.1016/j.aquatox.2012.01.018> PMID: 22343466
58. Foldbjerg R, Jiang X, Mieläus T, Chen C, Autrup H, Beer C. Silver nanoparticles—wolves in sheep's clothing? *Toxicol Res*. 2015; 4(3):563–75. <https://doi.org/10.1039/C4TX00110A>.
59. Rai M, Kon K, Ingle A, Duran N, Galdiero S, Galdiero M. Broad-spectrum bioactivities of silver nanoparticles: the emerging trends and future prospects. *Appl Microbiol Biotechnol*. 2014; 98(5):1951–61. <https://doi.org/10.1007/s00253-013-5473-x> PMID: 24407450

60. Benelli G. Mode of action of nanoparticles against insects. *Environ Sci Pollut Res Int.* 2018; 25(13):12329–41. <https://doi.org/10.1007/s11356-018-1850-4> PMID: 29611126
61. Nel A, Xia T, Mädler L, Li N. Toxic potential of materials at the nanolevel. *Science.* 2006; 311(5761):622–7. <https://doi.org/10.1126/science.1114397> PMID: 16456071
62. Wise JP Sr., Goodale BC, Wise SS, Craig GA, Pongan AF, Walter RB, et al. Silver nanospheres are cytotoxic and genotoxic to fish cells. *Aquat Toxicol.* 2010; 97(1):34–41. <https://doi.org/10.1016/j.aquatox.2009.11.016> PMID: 20060603
63. Ahamed M. Toxic response of nickel nanoparticles in human lung epithelial A549 cells. *Toxicol In Vitro.* 2011; 25(4):930–6. <https://doi.org/10.1016/j.tiv.2011.02.015> PMID: 21376802
64. Siddiqui MA, Ahamed M, Ahmad J, Majeed Khan MA, Musarrat J, Al-Khedhairi AA, et al. Nickel oxide nanoparticles induce cytotoxicity, oxidative stress and apoptosis in cultured human cells that is abrogated by the dietary antioxidant curcumin. *Food Chem Toxicol.* 2012; 50(3–4):641–7. <https://doi.org/10.1016/j.fct.2012.01.017> PMID: 22273695
65. Wilczek G, Babczynska A, Migula P, Wencelis B. Activity of Esterases as Biomarkers of Metal Exposure in Spiders from the Metal Pollution Gradient. *Polish J Environ Studies.* 2003; 12(6):765–72
66. Yan B, Wang L, Li Y, Liu N, Wang Q. Effects of cadmium on hepatopancreatic antioxidant enzyme activity in freshwater crab *Sinopotamon yangtsekiense*. *Acta Zool Sin.* 2007; 6:1121–8647147
67. Yousef HA, Abdelfattah EA, Augustyniak M. Antioxidant enzyme activity in responses to environmentally induced oxidative stress in the 5th instar nymphs of *Aiolopus thalassinus* (Orthoptera: Acrididae). *Environ Sci Pollut Res Int.* 2019; 26(4):3823–33. <https://doi.org/10.1007/s11356-018-3756-6> PMID: 30539392
68. Lijun L, Xuemei L, Yaping G, Enbo M. Activity of the enzymes of the antioxidative system in cadmium-treated *Oxya chinensis* (Orthoptera Acridoidea). *Environ Toxicol Pharmacol.* 2005; 20(3):412–6. <https://doi.org/10.1016/j.etap.2005.04.001> PMID: 21783620
69. Xia T, Kovochich M, Liong M, Mädler L, Gilbert B, Shi H, et al. Comparison of the mechanism of toxicity of zinc oxide and cerium oxide nanoparticles based on dissolution and oxidative stress properties. *ACS Nano.* 2008; 2(10):2121–34. <https://doi.org/10.1021/nn800511k> PMID: 19206459
70. Abdollahi M, Ranjbar A, Shadnia S, Nikfar S, Rezaie A. Pesticides and oxidative stress: a review. *Med Sci Monit.* 2004; 10(6):Ra141–715173684 PMID: 15173684
71. Cruz-Landim C. Origin of the peritrophic membrane of the adult *Apis mellifera* L. (Hymenoptera: Apidae). *Rev Brasil Biol.* 1985; 45(3):207–19
72. El-Saad AM, Kheirallah DA, El-Samad LM. Biochemical and histological biomarkers in the midgut of *Apis mellifera* from polluted environment at Beheira Governorate, Egypt. *Environ Sci Pollut Res Int.* 2017; 24(3):3181–93. <https://doi.org/10.1007/s11356-016-8059-1> PMID: 27864738
73. Rawi SM, Bakry FA, Al-Hazmi MA. Biochemical and histopathological effect of crude extracts on *Spodoptera littoralis* larvae. *J Evolut Biol Res.* 2011; 3(5):67–78. <https://doi.org/10.5897/JEBR.9000001>.
74. Younes M, Abou El Ela R, El-Mhasen M. Histopathological effects of some insecticides on the larval midgut and integument of the lesser cotton leafworm *Spodoptera exigua* (HB)(Lepidoptera: Noctuidae). *J Egypt Germ Soc Zool.* 2000; 32(E):19–32
75. Adel MM, El-Hawary FM, Abdel-Aziz NF, Sammour EA. Some physiological, biochemical and histopathological effects of *Artemisia monosperma* against the cotton leafworm, *Spodoptera littoralis*. *Arch Phytopathol Plant Protect.* 2010; 43(11):1098–110. <https://doi.org/10.1080/03235400802285562>.
76. Mokhamer ELHM, M.Elsamad DL, Elsayed DWO, L. Shonouda DM, Ali A. The ground beetle *Blaps polycresta* (Coleoptera:tenebrionidae) as Bioindicator of Heavy metals Soil Pollution. *J Adv Biol.* 2015; 7(1):1153–60. <https://doi.org/10.1007/s11356-015-4606-4> PMID: 25963070
77. Banumathi B, Vaseeharan B, Ishwarya R, Govindarajan M, Alharbi NS, Kadaikunnan S, et al. Toxicity of herbal extracts used in ethno-veterinary medicine and green-encapsulated ZnO nanoparticles against *Aedes aegypti* and microbial pathogens. *Parasitol Res.* 2017; 116(6):1637–51. <https://doi.org/10.1007/s00436-017-5438-6> PMID: 28389893
78. Al-Dhafar ZM, Sharaby A. Effect of zinc sulfate against the red palm weevil *Rhynchophorus ferrugineus* with reference to their histological changes on the larval midgut and adult reproductive system. *J Agricult Sci Technol.* 2012; 2(7A):888–936. <https://doi.org/10.17265/2161-6256/2012.07A.006>.
79. Cid A, Picado A, Correia JB, Chaves R, Silva H, Caldeira J, et al. Oxidative stress and histological changes following exposure to diamond nanoparticles in the freshwater Asian clam *Corbicula fluminea* (Müller, 1774). *J Hazard Mater.* 2015; 284:27–34. <https://doi.org/10.1016/j.jhazmat.2014.10.055> PMID: 25463214
80. Krishnan N, Kodrik D, Kludkiewicz B, Sehnal F. Glutathione-ascorbic acid redox cycle and thioredoxin reductase activity in the digestive tract of *Leptinotarsa decemlineata* (Say). *Insect Biochem Mol Biol.* 2009; 39(3):180–8. <https://doi.org/10.1016/j.ibmb.2008.11.001> PMID: 19049872

81. Krishnan N, Kodrik D. Antioxidant enzymes in *Spodoptera littoralis* (Boisduval): are they enhanced to protect gut tissues during oxidative stress? *J Insect Physiol.* 2006; 52(1):11–20. <https://doi.org/10.1016/j.jinsphys.2005.08.009> PMID: 16242709
82. Terra WR, Espinoza-Fuentes FP, Ribeiro AF, Ferreira C. The larval midgut of the housefly (*Musca domestica*): Ultrastructure, fluid fluxes and ion secretion in relation to the organization of digestion. *J Insect Physiol.* 1988; 34(6):463–72. [https://doi.org/10.1016/0022-1910\(88\)90187-4](https://doi.org/10.1016/0022-1910(88)90187-4).
83. Terra W. Evolution and function of insect peritrophic membrane. *Ciência Cult.* 1996; 48:317–24
84. Grewal SI, Jia S. Heterochromatin revisited. *Nat Rev Genet.* 2007; 8(1):35–46. <https://doi.org/10.1038/nrg2008> PMID: 17173056
85. Häcker G. The morphology of apoptosis. *Cell Tissue Res.* 2000; 301(1):5–17. <https://doi.org/10.1007/s004410000193> PMID: 10928277
86. Silva-Zacarin EC, Taboga SR, Silva de Moraes RL. Nuclear alterations associated to programmed cell death in larval salivary glands of *Apis mellifera* (Hymenoptera: Apidae). *Micron.* 2008; 39(2):117–27. <https://doi.org/10.1016/j.micron.2006.12.001> PMID: 17251032
87. Trump BF, Berezesky IK, Chang SH, Phelps PC. The pathways of cell death: oncosis, apoptosis, and necrosis. *Toxicol Pathol.* 1997; 25(1):82–8. <https://doi.org/10.1177/019262339702500116> PMID: 9061857
88. Pazir M, Afsharnasab M, Jalali Jafari B, Sharifpour I, Motalebi A, Dashtiannasab A. Detection and identification of white spot syndrome virus (WSSV) and infectious hypodermal and hematopoietic necrosis virus (IHHNV) of *Litopenaus vannamei* from Bushehr and Sistan and Baluchestan provinces (Iran), during 2009–2010. *Iran J Fisher Sci.* 2011; 10(4):708–26
89. Rodrigues A, Cunha L, Amaral A, Medeiros J, Garcia P. Bioavailability of heavy metals and their effects on the midgut cells of a phytophagous insect inhabiting volcanic environments. *Sci Total Environ.* 2008; 406(1):116–22. <https://doi.org/10.1016/j.scitotenv.2008.07.069> PMID: 18793793
90. Braeckman B. Heavy metal toxicity in an insect cell line (methyl-HgCl, HgCl₂, CdCl₂ and CuSO₄). In: Banfalvi G, (ed). *Cellular Effects of Heavy Metals.* New York: Springer; 2011. 115–44.
91. Risso-de Faverney C, Orsini N, de Sousa G, Rahmani R. Cadmium-induced apoptosis through the mitochondrial pathway in rainbow trout hepatocytes: involvement of oxidative stress. *Aquat Toxicol.* 2004; 69(3):247–58. <https://doi.org/10.1016/j.aquatox.2004.05.011> PMID: 15276330
92. Luzio A, Monteiro SM, Fontainhas-Fernandes AA, Pinto-Carnide O, Matos M, Coimbra AM. Copper induced upregulation of apoptosis related genes in zebrafish (*Danio rerio*) gill. *Aquat Toxicol.* 2013; 128–129:183–9. <https://doi.org/10.1016/j.aquatox.2012.12.018> PMID: 23314331
93. Polidori C, Pastor A, Jorge A, Pertusa J. Ultrastructural Alterations of Midgut Epithelium, But Not Greater Wing Fluctuating Asymmetry, in Paper Wasps (*Polistes dominula*) from Urban Environments. *Microsc Microanal.* 2018; 24(2):183–92. <https://doi.org/10.1017/S1431927618000107> PMID: 29560839
94. Cavados CF, Majerowicz S, Chaves JQ, Araújo-Coutinho CJ, Rabinovitch L. Histopathological and ultrastructural effects of delta-endotoxins of *Bacillus thuringiensis* serovar israelensis in the midgut of *Simulium pertinax* larvae (Diptera, Simuliidae). *Mem Inst Oswaldo Cruz.* 2004; 99(5):493–8. <https://doi.org/10.1590/s0074-02762004000500006> PMID: 15543412
95. Stern ST, Adisheshaiah PP, Crist RM. Autophagy and lysosomal dysfunction as emerging mechanisms of nanomaterial toxicity. *Part Fibre Toxicol.* 2012; 9:20. <https://doi.org/10.1186/1743-8977-9-20> PMID: 22697169
96. Česen MH, Pegan K, Spes A, Turk B. Lysosomal pathways to cell death and their therapeutic applications. *Exp Cell Res.* 2012; 318(11):1245–51. <https://doi.org/10.1016/j.yexcr.2012.03.005> PMID: 22465226
97. Repnik U, Stoka V, Turk V, Turk B. Lysosomes and lysosomal cathepsins in cell death. *Biochim Biophys Acta.* 2012; 1824(1):22–33. <https://doi.org/10.1016/j.bbapap.2011.08.016> PMID: 21914490
98. Triebkorn R, Köhler HR. The impact of heavy metals on the grey garden slug, *Deroceras reticulatum* (Müller): Metal storage, cellular effects and semi-quantitative evaluation of metal toxicity. *Environ Pollut.* 1996; 93(3):327–43. [https://doi.org/10.1016/s0269-7491\(96\)00048-6](https://doi.org/10.1016/s0269-7491(96)00048-6) PMID: 15093530
99. Köhler HR. Localization of metals in cells of saprophagous soil arthropods (Isopoda, Diplopoda, Collembola). *Microsc Res Tech.* 2002; 56(5):393–401. <https://doi.org/10.1002/jemt.10039> PMID: 11877814
100. Pigino G, Migliorini M, Paccagnini E, Bernini F. Localisation of heavy metals in the midgut epithelial cells of *Xenillus tegeocranus* (Hermann, 1804) (Acari: Oribatida). *Ecotoxicol Environ Saf.* 2006; 64(3):257–63. <https://doi.org/10.1016/j.ecoenv.2005.12.012> PMID: 16460803

101. Karpeta-Kaczmarek J, Augustyniak M, Rost-Roszkowska M. Ultrastructure of the gut epithelium in *Acheta domesticus* after long-term exposure to nanodiamonds supplied with food. *Arthropod Struct Dev.* 2016; 45(3):253–64. <https://doi.org/10.1016/j.asd.2016.02.002> PMID: 26921817
102. Nel AE, Mädler L, Velegol D, Xia T, Hoek EM, Somasundaran P, et al. Understanding biophysico-chemical interactions at the nano-bio interface. *Nat Mater.* 2009; 8(7):543–57. <https://doi.org/10.1038/nmat2442> PMID: 19525947
103. Moore MN. Do nanoparticles present ecotoxicological risks for the health of the aquatic environment? *Environ Int.* 2006; 32(8):967–76. <https://doi.org/10.1016/j.envint.2006.06.014> PMID: 16859745
104. Meyer JN, Leung MC, Rooney JP, Sandoel A, Hengartner MO, Kisby GE, et al. Mitochondria as a target of environmental toxicants. *Toxicol Sci.* 2013; 134(1):1–17. <https://doi.org/10.1093/toxsci/kft102> PMID: 23629515
105. Braeckman B, Brys K, Rzeznik U, Raes H. Cadmium pathology in an insect cell line: ultrastructural and biochemical effects. *Tissue Cell.* 1999; 31(1):45–53. <https://doi.org/10.1054/tice.1998.0019> PMID: 18627852
106. Cheville N. *Ultrastructural Pathology: The Comparative Cellular Basis of Disease.* Hoboken: John Wiley & Sons; 2009.
107. Belyaeva EA, Dymkowska D, Wieckowski MR, Wojtczak L. Mitochondria as an important target in heavy metal toxicity in rat hepatoma AS-30D cells. *Toxicol Appl Pharmacol.* 2008; 231(1):34–42. <https://doi.org/10.1016/j.taap.2008.03.017> PMID: 18501399
108. Schönthal AH. Endoplasmic reticulum stress: its role in disease and novel prospects for therapy. *Scientifica (Cairo).* 2012; 2012:857516. <https://doi.org/10.6064/2012/857516> PMID: 24278747
109. Braunbeck T, Volkl A. Toxicant-induced cytological alterations in fish liver as biomarkers of environmental pollution? A case study on hepatocellular effects of dinitro-*o*-cresolin golden ide (*Leuciscus idus melanotus*). In: Braunbeck T, Hanke W, Segner H, (eds). *Fish Ecotoxicology and Ecophysiology.* Germany: Weinheim; 1993. 55–80. PMID: 8339279
110. Proskuryakov SY, Konoplyannikov AG, Gabai VL. Necrosis: a specific form of programmed cell death? *Exp Cell Res.* 2003; 283(1):1–16. [https://doi.org/10.1016/s0014-4827\(02\)00027-7](https://doi.org/10.1016/s0014-4827(02)00027-7) PMID: 12565815
111. Elmore S. Apoptosis: a review of programmed cell death. *Toxicol Pathol.* 2007; 35(4):495–516. <https://doi.org/10.1080/01926230701320337> PMID: 17562483